MMLIBB DC-DC Converter: A Novel Modular, Multi-Level, Interleaved-Based, Bidirectional Topology

Vitor Monteiro
Centro ALGORITMI
University of Minho
Guimaraes, Portugal
vmonteiro@dei.uminho.pt

Joao L. Afonso
Centro ALGORITMI
University of Minho
Guimaraes, Portugal
jla@dei.uminho.pt

***Abstract*—The extent of applications that claims the use of power electronics systems is cumulative, deriving innovative topologies from the classical topologies, and diversifying the requisites for innovative topologies, such as the need for multiple inputs/outputs. In addition, prerequisites such as high efficiency, modularity, bidirectionality, low ripple, high voltage and/or high current interfaces, high frequency, and low cost are pushing the necessity of new power electronics topologies. Aligned with this vision, a new topology is proposed. Due to its structure, the modular, multi-level, interleaved-based, bidirectional (MMLIBB) DC-DC converter topology can be utilized for various purposes, such as the interface of renewables and/or energy storage elements with multiple DC interfaces and hybrid AC/DC grids. The MMLIBB topology operates in bidirectional mode and has a modular structure, which easily incorporates additional sub-modules for increasing the number of DC interfaces. Likewise, as the number of added sub-modules increases, the number of multilevel voltages rises, and the ripple current declines. The proposed topology can operate with the classical current or voltage control, though the modulation must be very specific, and hence, a comprehensive attention is given to that in this paper. The characteristics of the MMLIBB topology are proven based on simulations obtained for decisive operating situations.**

***Keywords*—MMLIBB DC-DC Converter, Modular, Multi-Level, Interleaved-Based, Bidirectional, Power Electronics.**

I. INTRODUCTION

Primarily since the initiation of this century, the instituted power grids are confronting the incorporation of numerous active and passive technologies, allowing a convergence for smart grids [1]. This progress, complemented by on-grid and off-grid concepts, is challenging even more the request for technological solutions based on power electronics systems, both in matters of topologies and algorithms. As examples, renewable energies (on-shore and off-shore), solid-state transformers, DC grids and electric mobility are essential pillars in this proceed and are assuming a leading importance [2][3]. Even so, other examples can be exhibited, e.g., small everyday low-power equipment is also requiring technological solutions of power electronics with further efficacy, features, and power density [4][5]. Similarly, result of this development and intending guaranteeing power quality, power electronics is likewise indispensable [6][7]. Very specifically within the whole domain topic of power converters, it is recognized that DC-DC converters are definitely indispensable as interface for almost all applications, where a distinct interest is also conferred for the growing DC grids.

DC-DC converters based on the grouping of an interleaved configuration with a single-input and multi-outputs is proposed in [8], while a modular DC-DC converter with input-series and output-series and offering isolation is offered in [9]. A multi-stage DC-DC with not many amounts of components and constituted by cells of inductor, capacitor, and two diodes is planned in [10]. A method of designing DC-DC converters based on a particular voltage gain, identified as an inverse problem is studied in [11]. In terms of control, distinct procedures can be engaged giving specific DC-DC converters, e.g., a sliding-mode control is projected in [12] for a DC-DC cascade boost, and direct model predictive control is offered in [13] for a DC-DC non-inverting buck-boost. Relatively to applications, the management control of multi-port DC-DC converters for stand-alone renewables-storage systems is proposed in [14], a non-isolated DC-DC converter for high-power functions is proposed in [15], a cascade modular multi-level composition carried by a DC-DC converter is proposed in [16], and an evaluation of non-isolated DC-DC converters for fuel-cell electric mobility applications is offered in [17]. Although the abundant topologies available and the ample applications, the innovation for DC-DC converters continues active and ranged with numerous matters, e.g., a detailed review about soft-switching techniques, including for DC-DC converters, is offered in [18], a unified approach for synthesis and analysis of non-isolated DC-DC converters is proposed in [19], a thorough view of high-gain DC-DC converters coordinated by coupled inductors and with voltage multipliers performances is proposed in [20], and the design and evaluation of a DC-DC converter based on a planar three-coupled inductors is proposed in [21].

A specialized multilevel bidirectional DC-DC converter was original proposed in [22], but with the intent of generating a DC grid in the interface with a solid-state transformer, so, only presenting four interfaces (three interfaces with the solid-state transformer and the other one with the DC-DC). Linked with this background, a novel modular, multi-level,

interleaved-based, and bidirectional topology, the MMLIBB DC-DC converter, is proposed in this paper, which suggestions as main notable feature a generalized modular design to be adapted for numerous requests in smart grids. As noticing features, it can be underlined: (a) the MMLIBB DC-DC converter can be constituted by several sub-modules, connected in a vertical cascade structure, for achieving the multi-level characteristic and, at the same time, multiple DC ports; (b) each DC interface has a split DC-link, which can be useful, e.g., for interfacing three-wire DC grids; (c) however, by applying a proper modulation, an interleaved-based operation can also be reached at the same time, giving an important characteristic with the intent of decreasing the size of passive filters; (d) in addition, the bidirectionality is also a possibility independently of the other characteristics (i.e., modular, multi-level, and interleaved-based); (e) the control can be performed with voltage or current feedback, independently of the modulation. A full comparison with other topologies is out of the scope, since the intent is to validate a topology.

Fig. 1 presents the MMLIBB DC-DC converter, where is displayed that each sub-module is created by four full-controlled switching devices (IGBTs) and by a split DC interface. The detailed operation principle is shown in section II, while the proposed modulation is established in section III. The validation for the key characteristics is presented in section IV and conclusions are provided in section V.

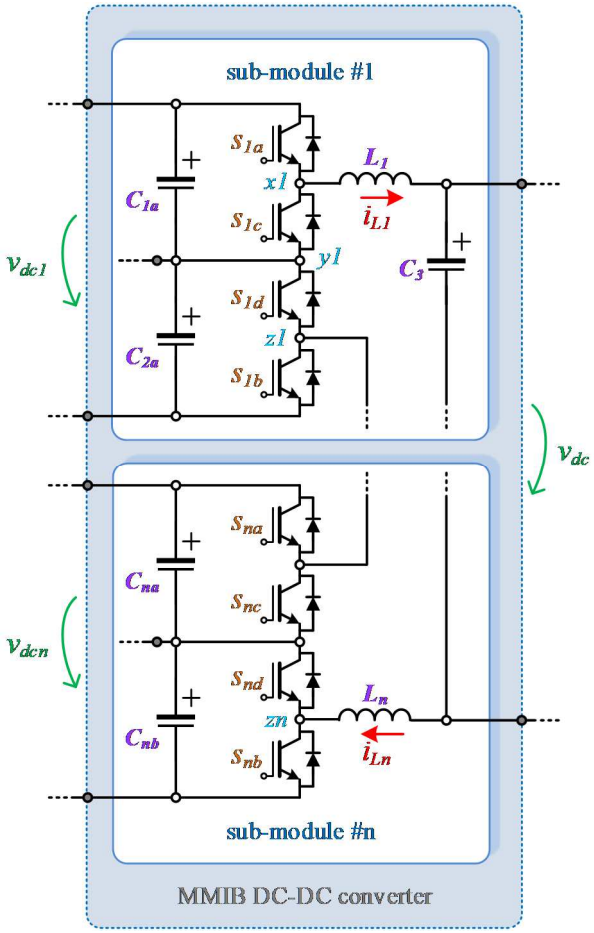

Fig. 1. Proposed MMLIBB DC-DC converter, mainly highlighting the modular structure and the consequent distinct DC interfaces.

II. MMLIBB DC-DC Converter: Operation Principle

The MMLIBB DC-DC converter is made up of several sub-modules that can be linked together in a cascade mode. Each sub-module is formed by a set of four IGBTs and a split DC-link that can be contemplated as a single DC-link or, if the application justifies it, as a split DC-link, e.g., on the interface of three-wire DC grids or solid-state transformers. Each sub-module can operate in buck or boost mode, and for that intention two IGBTs are switched in each mode. During buck operation s_{nA} and s_{nB} and during boost operation s_{nC} and s_{nD}. Furthermore, the control signals of each IGBT are offset from each other (i.e., a phase angle of ϕ), whose offset value depends on the number of sub-modules (SM) considered, according to:

$$\phi_{snA,B} = \frac{360}{2\,SM}. \tag{1}$$

Obviously, the IGBTs are switched individually, i.e., no control signal is shared by two IGBTs. Though, the control signals of each IGBT can be active ON or OFF at the same time or not. The condition for this is dependent on buck or boost working and input and output voltage. Table I shows the viable states.

Table I. Possible control states for each IGBT.

	state				voltage	
	s_{nA}	s_{nB}	s_{nC}	s_{nD}	v_{xnyn}	v_{ynzn}
buck	ON	OFF	OFF	OFF	$v_{dc}/2$	0
	OFF	ON	OFF	OFF	0	$v_{dc}/2$
	OFF	OFF	OFF	OFF	0	0
	ON	ON	OFF	OFF	$v_{dc}/2$	$v_{dc}/2$
boost	OFF	OFF	ON	OFF	0	$v_{dc}/2$
	OFF	OFF	OFF	ON	$v_{dc}/2$	0
	OFF	OFF	ON	ON	0	0
	OFF	OFF	OFF	OFF	$v_{dc}/2$	$v_{dc}/2$

To achieve the control signals, it is necessary to resort to an exact modulation strategy, subsequently, several carrier signals (C_{PWM}) are reflected according to the number of sub-modules contemplated, conferring to:

$$c_{PWM} = 4\,SM\,. \tag{2}$$

Since the offset concerning carriers is given by the value resulting from equation (1), in this way, the IGBTs are switched individually and with a fixed frequency, and the comparison signal with the various carriers comes from the control, which can be with current control or with voltage control. The suggested modulation does not depend on the voltage or current control tactic that can be adopted. Thus, it is feasible to declare a control in which the ripple of the controlled variable admits a frequency ($f_{\Delta iL}$) multiple of the number of sub-modules and the individual switching frequency of each IGBT (f_{sw}), relating to:

$$f_{\Delta iL} = 2\,SM\,f_{sw}\,. \tag{3}$$

Hence, there is an interleaved-based operation with the worthy benefit of drastically cutting the dimensions of the passive coupling components, even without the need to connect

converters in parallel (i.e., as with classic interleaved assemblies). It is vital to remark that this operation is guaranteed even if the voltage values in each sub-module are not the same. The average value of the current/voltage in the IGBTs is, respectively:

$$\overline{i}_{sn\{C,D\}} = \overline{i_{L_{\{1,n\}}}} \frac{v_{dc1}}{SM\ v_{dcn}}, \tag{4}$$

$$\overline{i}_{sn\{A,B\}} = \overline{i_{L_{\{1,n\}}}} - \overline{i}_{sn\{C,D\}}, \tag{5}$$

$$\overline{v}_{sn\{A,B\}} = 0.5\left(v_{dc1} - \frac{v_{dcn}}{SM^2}\right) SM, \tag{6}$$

$$\overline{v}_{s\{C,D\}} = \left(v_{dc1} - \frac{v_{dcn}}{4}\right) SM^{-1}. \tag{7}$$

To undertaking a right balance between voltages and currents, the voltage in each sub-module should be twice the voltage in the output/input. Besides, in such case, the ripple is cancelled. By adjusting the value of voltages, the MMLIBB DC-DC converter can be forced to operate in this mode.

III. MMLIBB DC-DC Converter: Modulation and Validation in Distinct Operations

The operating validation of the MMLIBB DC-DC converter was approved using a PSIM simulation model. To get a proof that permits to attest all the potentialities of the proposed converter, four sub-modules were considered. For the switching frequency a value of 20 kHz was specified and for the passive coupling filters a value of 500 µH. As a sampling frequency for the control, implemented in C language, a value of 40 kHz was stipulated. For the voltages at every interface, several values were contemplated to acquire a more extensive validation, as indicated in the thereafter results.

Fig. 2 displays all the carriers and all the control signals of the IGBTs during buck action, indicating a representative operation. Perceptibly, as described in the previous sections, the carriers are not synchronized with the same phase, but they present a phase shift corresponding to 360 degrees divided by twice the number of sub-modules, in this case resulting in a value of 45 degrees (equation (1)). Hence, e.g., for the first sub-module, accepting that the first carrier is in phase 0 degrees, the second carrier is in phase 45 degrees, and subsequently for the others. Hence, the control signals have, respectively, the same offset.

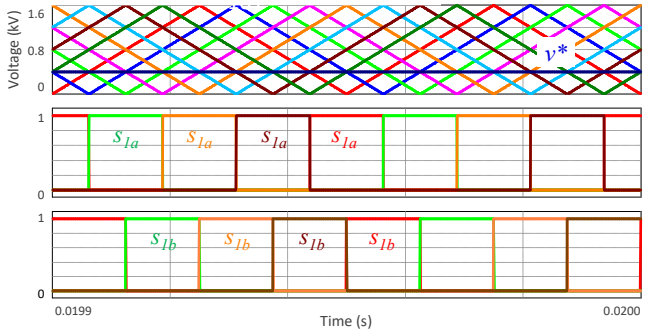

Fig. 2. Carriers and all the control signals of the IGBTs during buck operation.

This condition is explicit in the result displayed in Fig. 3, where the signals resultant from the comparison are verified. This principle of activity is valid for any sub-module. Obviously, by adding more sub-modules, the delay between carriers and the respective control signals will be greater. As this is a buck function, the control signal accepts a positive value when the reference is greater than the carrier and a null value when it is less.

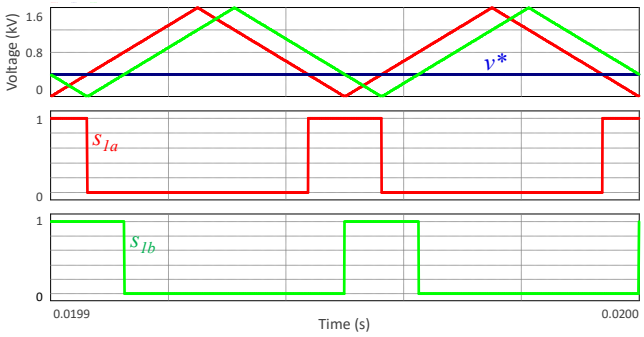

Fig. 3. Signals resulting from the comparison of the reference signal with the carriers for the buck operation.

This operating criterion is the same for any sub-module, so, for the case in question in which four sub-modules are considered, the signals have a 45 degrees offset angle between them, starting at 0 and until reaching 360 degrees. This situation is shown in the result of Fig. 4. Evidently, the remaining IGBTs are OFF when operating in buck.

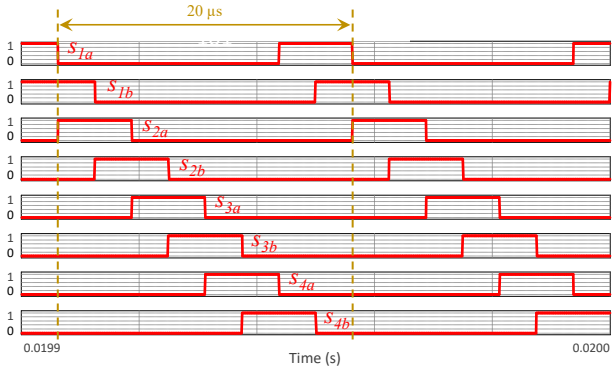

Fig. 4. Control signals for the IGBTs during the buck operation.

When a current control plan is employed, the principal properties of the MMLIBB DC-DC converter are proved (in this case, based on predictive control), and which make it appealing for a varied selection of applications. Thus, Fig. 5 reveals the current for a reference of 10 A, considering an output voltage with a value of 400 V that is twice the value of the input voltage of each sub-module. This result is exhibited with such values to suggest that, under such operating restrictions, the current ripple does not exist and that, distinctly, the current follows the established reference.

If the voltage values and circumstances remain the same, even if the current reference varies, the current follows such variations, continuously maintaining a zero ripple. This situation is feasible to achieve, even in the transition moment, because the converter is forced to change the voltage levels at

which it is operating, as can be appreciated in the result proved in Fig. 6. In this instance, the current doubled and the converter operated with five voltage levels. After the transition, the converter continues to operate with zero current ripple and with the same voltage levels, since the values of the input and output voltages did not change. This kind of operation can correspond, e.g., to applications using batteries charged with different currents that vary abruptly (e.g., regenerative braking in electric mobility). This operation is noted in Fig. 7, confirming that the current diverges approximately instantaneously with its reference, evidently not being the same.

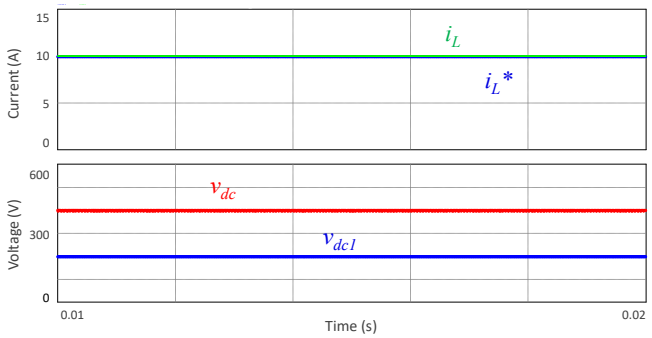

Fig. 5. Current for a reference of 10 A, considering an output voltage with a value of 400 V that is twice the value of the input voltage of each sub-module (200 V).

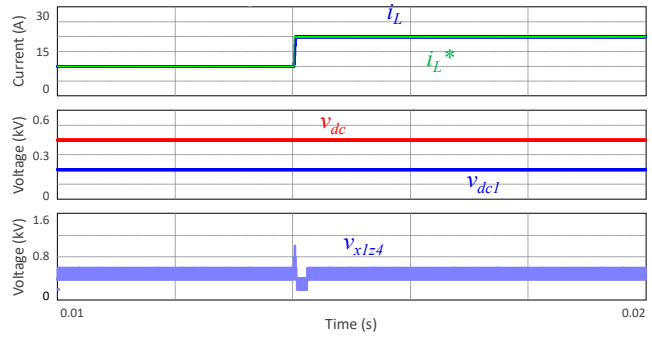

Fig. 6. Transient state of the current changing from 10 A to 20 A, maintaining an output voltage with a value of 400 V that is twice the value of the input voltage of each sub-module (200 V), verifying the multi-level voltage transition.

On the other hand, altering the voltage value, e.g., dropping the output voltage value to a value lower than the voltage of each sub-module, perceptibly, the current ripple is no longer null and starts to assume a value proportional to the difference in voltages between the input and the voltage of each sub-module. Still, the current ripple has a frequency that matches the IGBT frequency multiplied by twice the number of sub-modules. Accordingly, for the case in question of four sub-modules, the ripple has a frequency of 160 kHz. This method is exceptionally beneficial when is needed to reduce the passive components (i.e., using an interleaved-based operation). This condition is illustrated in Fig. 8, where the voltage of the converter does not accept as many values as in the case offered before, because the values of the output voltages and of each sub-module are different, although they remain with the same value even with the change of voltage. The note proving the correlation between the frequencies (switching and current ripple) is shown in Fig. 9, where the current absolutely follows its reference.

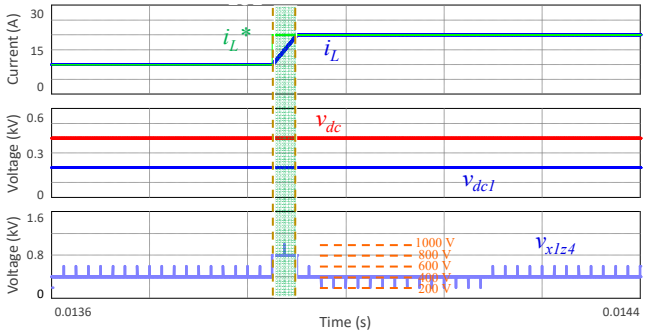

Fig. 7. Detail of the transient state of the current changing from 10 A to 20 A, verifying the multi-level voltage (assuming five distinct values) during the transition.

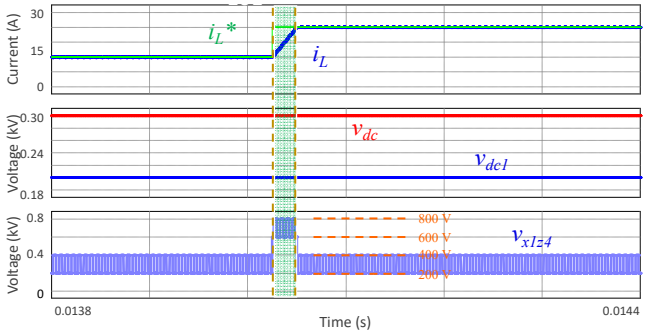

Fig. 8. Transient state of the current changing from 10 A to 20 A, with output voltage of 300 V and input voltage of each sub-module of 200 V, verifying the multi-level voltage transition and the ripple presented in the current.

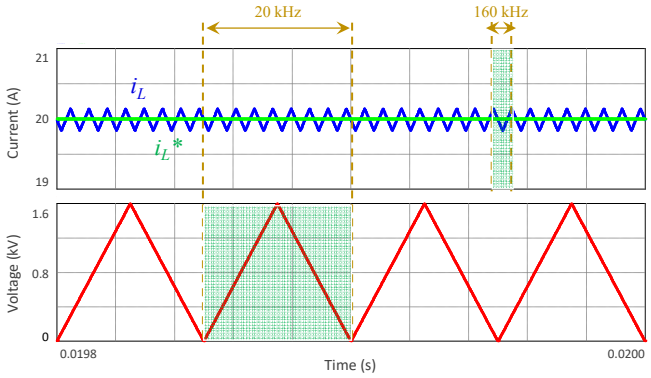

Fig. 9. Detail showing the relationship between the switching frequency and the frequency of the current ripple in buck mode.

If instead of a voltage with a fixed value at the output (e.g., a battery), a resistive load is considered and the current reference is progressively expanded, noticeably, the voltage also expands. Hence, expanding the output voltage forces the converter voltage to adopt another value, changing the value at every half of the voltage value in each sub-module. In this case, as indicated in Fig. 10, the nine voltage values are visible.

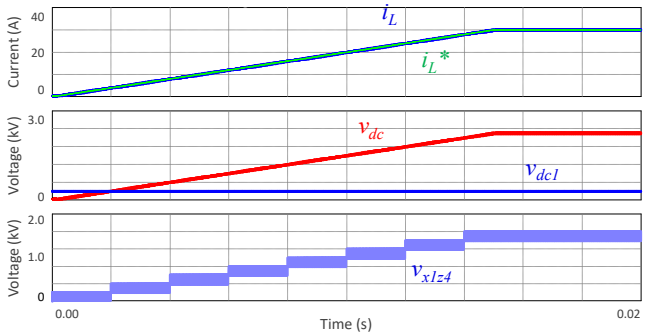

Fig. 10. Transient state of the current changing from 0 A to 30 A, and the output voltage changing from 0 V to 1500 V, with the input voltage of each sub-module of 200 V, verifying the multi-level voltage transition (nine voltage levels) and the ripple presented in the current.

The earlier cases refer to the operation in buck, but the operation in boost is not very distinct. Fig. 11 displays the carriers and control signals of the IGBTs of one of the sub-modules, also authenticating that the offset is 45 degrees, where the control signal assumes a positive value when the reference signal is smaller than the carrier, and the opposite happens when the reference signal is higher than the carrier.

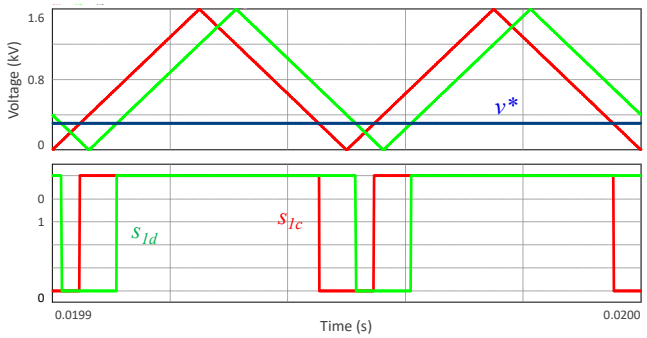

Fig. 11. Signals resulting from the comparison of the reference signal with the carriers for the boost operation.

Fig. 12 reveals all the IGBT control signals in boost mode, with 45 degrees offset between each control signal. The lasting IGBTs are in OFF mode during boost. In addition, it is proven that the current arises its reference regardless of the voltage values, as checked in Fig. 13. In this instance, an input voltage value lower than the voltage of each sub-module was contemplated. The current is revealed with a negative value for the reason that it is the position of the sensor. Also in this case, the voltage levels of the converter are exposed, and they vary giving to the operating settings. As for buck, the current has zero ripple when the input voltage is equal to the voltage of each sub-module and undertakes a distinct value when these voltages also alter. In these states, again, the current ripple has a frequency of 160 kHz as evidenced in Fig. 14.

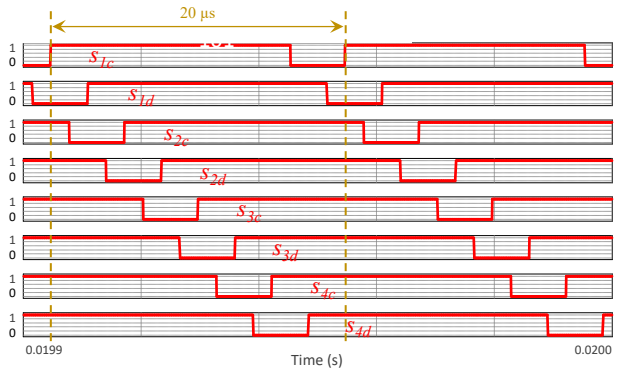

Fig. 12. Control signals for the IGBTs during the boost operation.

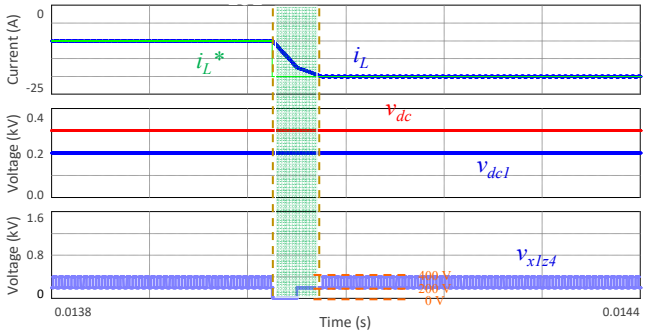

Fig. 13. Transient state of the current changing from 10 A to 20 A with input voltage of 300 V and output voltage at each sub-module of 200 V, verifying the multi-level voltage transition and the ripple presented in the current.

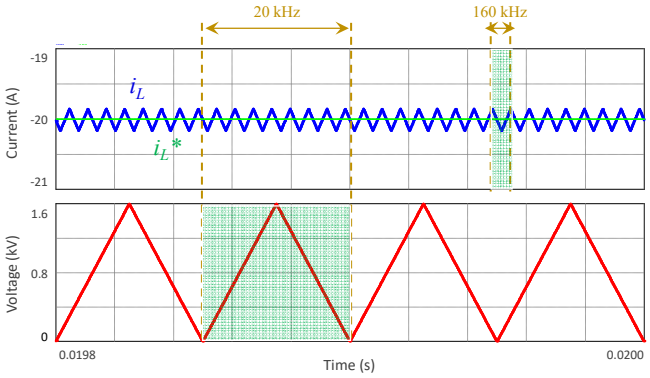

Fig. 14. Detail showing the relationship between the switching frequency and the frequency of the current ripple in boost mode.

IV. Conclusions

Power electronics is unequivocally indispensable for the development of more innovative applications for smart grids. In this paper, a novel modular, multi-level, interleaved-based, bidirectional (MMLIBB) DC-DC converter topology is proposed, which have precise characteristic to be used in exceptional applications, e.g., that requires multiple DC interfaces. The modular structure was explained, and it was depicted that expanding the number of sub-modules, expands the number of DC interfaces, the number of voltage levels (i.e., multilevel feature), and the ripple frequency (i.e., interleaved-based feature). Along with the paper, the proof through simulations exhibits the bidirectional operation, in

buck mode from the sub-modules to the main DC interface, or in boost mode from the main DC interface to the sub-modules. In addition, for a MMLIBB topology based on four sub-modules, it was tested that the current has no ripple when the voltage in the main DC interface is equal to the double of the voltage in each sub-module, and that it is independent of the current control both for operation in steady and transient state. When such voltage condition does not happen, it was verified that the current ripple present a frequency with a value eight-times greater than the switching frequency. Besides, the operation with multilevel voltages (nine levels) was proven for both steady and transient state.

ACKNOWLEDGMENT

This work has been supported by FCT – Fundação para a Ciência e Tecnologia within the R&D Units Project Scope: UIDB/00319/2020.

REFERENCES

[1] N. Ahmad, Y. G. Ghadi, M. Adnan, M. Ali, "From Smart Grids to Super Smart Grids: A Roadmap for Strategic Demand Management for Next Generation SAARC and European Power Infrastructure," IEEE Access, vol.11, pp.12303-12341, 2023.

[2] L. Zheng et al., "Solid-State Transformer and Hybrid Transformer With Integrated Energy Storage in Active Distribution Grids: Technical and Economic Comparison, Dispatch, and Control," IEEE Journal of Emerging and Selected Topics in Power Electronics, vol.10, no.4, pp.3771-3787, Aug. 2022.

[3] Vitor Monteiro, J. Ferreira, A. Melendez, C. Couto, Joao L. Afonso, "Experimental Validation of a Novel Architecture Based on a Dual Stage Converter for Off-Board Fast Battery Chargers of Electric Vehicles," IEEE Trans. Veh. Tech., vol.67, pp.1000-1011, Feb. 2018.

[4] F. Blaabjerg, J. M. Guerrero, "Smart Grid and Renewable Energy Systems," ICEMS International Conference on Electrical Machines and Systems, pp.1-10, Aug. 2011.

[5] A. R. Zamani, M. Parsa Moghaddam, M. R. Haghifam, "Evaluating the Impact of Connectivity on Transactive Energy in Smart Grid," IEEE Trans. Smart Grid, vol.13, no.3, pp.2491-2494, May 2022.

[6] A. G. S. Chawda, A. G. Shaik, "Power Quality Improvement in Rural Grid Using Adaptive Control Algorithm to Enhance Wind Energy Penetration Levels," IEEE Trans. Smart Grid, vol.14, no.3, pp.2075-2084, May 2023.

[7] V. Monteiro et al., "A Novel Three-Phase Multi-Objective Unified Power Quality Conditioner," IEEE Trans. Industrial Electronics (accepted for publication), 2023.

[8] E. Aranda, S. Litrán, M. Prieto, "Combination of interleaved single-input multiple-output DC-DC converters," CSEE Journal of Power and Energy Systems, vol.8, no.1, pp.132-142, Jan. 2022.

[9] A. Bottion, I. Barbi, "Input-Series and Output-Series Connected Modular Output Capacitor Full-Bridge PWM DC–DC Converter," IEEE Trans. Ind. Electron., vol.62, no.10, pp.6213-6221, Oct. 2015.

[10] G. Kumar, M. Sai Krishna, S. Kumaravel, E. Babaei, "Multi-Stage DC-DC Converter Using Active LC2D Network With Minimum Component," IEEE Trans. Circuits and Systems II: Express Briefs, vol.68, no.3, pp.943-947, March 2021.

[11] R. Panigrahi, S. Mishra, A. Joshi, K. Ngo, "DC-DC Converter Synthesis: An Inverse Problem," IEEE Trans. Power Electron., vol.35, no.12, pp.12633-12638, Dec. 2020.

[12] S. Chincholkar, W. Jiang, C. Chan, "A Normalized Output Error-Based Sliding-Mode Controller for the DC–DC Cascade Boost Converter," IEEE Trans. Circuits and Systems II: Express Briefs, vol.67, no.1, pp.92-96, Jan. 2020.

[13] B. Ullah, H. Ullah, S. Khalid, "Direct Model Predictive Control of Noninverting Buck-boost DC-DC Converter," CES Trans. Electrical Machines and Systems, vol.6, no.3, pp.332-339, Sept. 2022.

[14] Y. Liang, H. Zhang, M. Du, K. Sun, "Parallel coordination control of multi-port DC-DC converter for stand-alone photovoltaic-energy storage systems," CPSS Trans. Power Electronics and Applications, vol.5, no.3, pp.235-241, Sept. 2020.

[15] G. Bastos, L. Costa, F. Tofoli, G. Bascopé, R. Bascopé, "Nonisolated DC–DC Converters with Wide Conversion Range for High-Power Applications," IEEE Journal of Emerging and Selected Topics in Power Electronics, vol.8, no.1, pp.749-760, Mar. 2020.

[16] H. Akagi, R. Kitada, "Control and Design of a Modular Multilevel Cascade BTB System Using Bidirectional Isolated DC/DC Converters," IEEE Trans. Power Electron., vol.26, no.9, pp.2457-2464, Sept. 2011.

[17] M. Sagar Bhaskar et al., "Survey of DC-DC Non-Isolated Topologies for Unidirectional Power Flow in Fuel Cell Vehicles," IEEE Access, vol.8, pp.178130-178166, 2020.

[18] S. Mohammed, J. Jung, "A State-of-the-Art Review on Soft-Switching Techniques for DC–DC, DC–AC, AC–DC, and AC–AC Power Converters," IEEE Trans. Ind. Informa., vol.17, no.10, pp.6569-6582, Oct. 2021.

[19] M. Gitau, G. Adam, L. Masike, M. Mbukani, "Unified Approach for Synthesis and Analysis of Non-Isolated DC-DC Converters," IEEE Access, vol.9, pp.120088-120109, 2021.

[20] L. Schmitz, D. Martins, R. Coelho, "Comprehensive Conception of High Step-Up DC–DC Converters with Coupled Inductor and Voltage Multipliers Techniques," IEEE Trans. Circuits and Systems I: Regular Papers, vol.67, no.6, pp.2140-2151, June 2020.

[21] T. Yao, W. Wang, "Analysis and Design of Three-End Planar Coupled Inductor Based DC–DC Converter," IEEE Journal of Emerging and Selected Topics in Industrial Electronics, vol.4, no.1, pp.28-36, Jan. 2023.

[22] Vítor Monteiro, Cátia F. Oliveira, João L. Afonso, "A Multilevel Bidirectional Four-Port DC-DC Converter to Create a DC-Grid in Solid-State Transformers with Hybrid AC/DC Grids," IEEE YEF-ECE International Young Engineers Forum, Portugal, pp.26-31, July 2021.